



Contents lists available at ScienceDirect

Intermetallics

journal homepage: [www.elsevier.com/locate/intermet](http://www.elsevier.com/locate/intermet)

# Enthalpy relaxation in $\text{Cu}_{46}\text{Zr}_{45}\text{Al}_7\text{Y}_2$ and $\text{Zr}_{55}\text{Cu}_{30}\text{Ni}_5\text{Al}_{10}$ bulk metallic glasses by differential scanning calorimetry (DSC)

J.C. Qiao, J.M. Pelletier\*

Université de Lyon, MATEIS, UMR CNRS5510, Bat. B. Pascal, INSA-Lyon, F-69621 Villeurbanne Cedex, France

## ARTICLE INFO

## Article history:

Received 8 April 2010

Received in revised form

27 August 2010

Accepted 31 August 2010

Available online xxx

## Keywords:

A. Intermetallics

B. Thermal properties

B. Glasses, metallic

E. Physical properties

## ABSTRACT

Structural relaxation process in  $\text{Cu}_{46}\text{Zr}_{45}\text{Al}_7\text{Y}_2$  and  $\text{Zr}_{55}\text{Cu}_{30}\text{Ni}_5\text{Al}_{10}$  bulk metallic glasses during annealing below the glass transition temperature  $T_g$  was investigated by differential scanning calorimetry (DSC). The features of enthalpy relaxation are sensitive to both annealing temperature and annealing time. For a given annealing time  $t_a$ , the results indicated that the relaxation time  $t_a$  decreases with increasing the annealing temperature  $T_a$ , in good agreement with results relative to other bulk metallic glasses. Additionally, the enthalpy relaxation behaviour of the bulk metallic glasses appears independent on the cooling rate used before the physical aging experiments, i.e. on the initial as-cast state. The recovered enthalpy evolution of the bulk metallic glasses is well described by the Kohlrausch–Williams–Watts (KWW) exponential relaxation function as  $\Delta H(T_a) = \Delta H_{eq}\{1 - \exp[-(t_a/\tau)^\beta]\}$ . Kohlrausch exponent  $\beta$  and enthalpy relaxation time  $\tau$  are sensitive to the composition of the bulk metallic glasses. Finally, the influence of different heating treatment processes on the enthalpy relaxation in the bulk metallic glasses is presented and shows that this phenomenon is mainly reversible. The structural relaxation behaviour is interpreted by free volume model and quasi-point defects model. Kinetic fragility parameters  $m$  in  $\text{Cu}_{46}\text{Zr}_{45}\text{Al}_7\text{Y}_2$  and  $\text{Zr}_{55}\text{Cu}_{30}\text{Ni}_5\text{Al}_{10}$  bulk metallic glasses are 72 and 69, respectively, indicating therefore that these alloys are intermediate glasses.

Crystallization process was also investigated by DSC experiments. According to the Kissinger model, corresponding activation energy is 3.18 eV in  $\text{Cu}_{46}\text{Zr}_{45}\text{Al}_7\text{Y}_2$ , and 3.19 eV in  $\text{Zr}_{55}\text{Cu}_{30}\text{Ni}_5\text{Al}_{10}$ , respectively.

© 2010 Elsevier Ltd. All rights reserved.

## 1. Introduction

Bulk metallic glasses have attracted considerable attention over the last decades, since they have excellent strength, outstanding stability and high mechanical properties [1–4]. They have been demonstrated as one of the promising materials for fabricating various micro-devices. In practical applications, physical properties and mechanical properties are always linked. In recent years, one of the main research topics about bulk metallic glasses is the structural relaxation occurring during physical aging. In bulk metallic glasses, when a heat treatment is performed below the glass transition temperature  $T_g$ , the structure of the bulk metallic glass tends to equilibrium or at least to a more stable state, but without occurrence of crystallization. This phenomenon, called structural relaxation, is observed not only in bulk metallic glasses, but also in other amorphous materials, like polymers or oxide glasses [5–13]. Structural relaxation is always associated with modifications of

mechanical properties, thermodynamics features, densities and transport properties [6].

The first investigations were performed in amorphous polymers [13,14]. Let us for instance mention the study reported by Vigier and Tatibouet [14] in PET (with many references included). They have shown that thermal and micromechanical properties of both amorphous and semi crystalline PET depend on aging effects induced by thermal treatments below  $T_g$ . The kinetics of the return to equilibrium of the specific enthalpy when isothermally aged below  $T_g$  has been interpreted using a physical model assuming diffusion and annihilation of defects (called quasi-point defects). This model takes into account the distribution in the mobility of these defects. The quasi-point defects model is based on the major assumption that density fluctuations in glassy polymers or amorphous solids could be considered as quasi-point defects [15–17].

In bulk metallic glasses, many researchers have used differential scanning calorimetry (DSC) to investigate the structural relaxation and the free volume model to describe their results, especially the kinetics of this evolution. Xu et al. [18] reported that based on the enthalpy change measurements and the equilibrium free volume at the onset temperature of glass transition, quantitative determination

\* Corresponding author. Tel.: +33 4 72 43 83 18; fax: +33 4 72 43 85 28.  
E-mail address: [jean-marc.pelletier@insa-lyon.fr](mailto:jean-marc.pelletier@insa-lyon.fr) (J.M. Pelletier).

of the free volume of Pd<sub>40</sub>Ni<sub>40</sub>P<sub>20</sub> bulk metallic glass is possible. Haruyama et al. [19] demonstrated that enthalpy relaxation data in Pd<sub>42.5</sub>Cu<sub>30</sub>Ni<sub>7.5</sub>P<sub>20</sub> bulk metallic glass and density relaxation data in Pd<sub>40</sub>Ni<sub>40</sub>P<sub>20</sub> bulk metallic glass could be well fitted by non-Debye relaxation function. Then, Haruyama research group has investigated the free volume evolution in detail [20–24]. Based on the density data obtained in a Pd<sub>40</sub>Ni<sub>40</sub>P<sub>20</sub> bulk metallic glass [20,21], they observed that the kinetics of free volume relaxation in sub-*T<sub>g</sub>* region could be well fitted by a stretched exponential relaxation function with a Kohlrausch exponent less than unity.

Many investigations concern Pd-based bulk metallic glasses, but also Zr-based and Cu-based bulk metallic glasses. For instance, Cu<sub>46</sub>Zr<sub>45</sub>Al<sub>7</sub>Y<sub>2</sub> [25–27] and Zr<sub>55</sub>Cu<sub>30</sub>Ni<sub>5</sub>Al<sub>10</sub> [28–30] BMG show excellent glass forming ability, wide super-cooled liquid region and high mechanical properties. The thermal properties of the two bulk metallic glasses are listed in Table 1: glass transition temperature (*T<sub>g</sub>*), temperature of the onset of crystallization (*T<sub>x</sub>*) and crystallization peak temperature (*T<sub>p</sub>*). These values are very similar for the two bulk metallic glasses. The structural relaxation in Zr<sub>55</sub>Cu<sub>30</sub>Al<sub>10</sub>Ni<sub>5</sub> bulk metallic glass was investigated by some researchers [31,32]. Haruyama et al. [31] reported the kinetics of structural relaxation in Zr<sub>55</sub>Cu<sub>30</sub>Al<sub>10</sub>Ni<sub>5</sub> bulk metallic glass. They give several interesting research results, for example, they observed a  $\alpha$ -relaxation-like behaviour in Zr<sub>55</sub>Cu<sub>30</sub>Al<sub>10</sub>Ni<sub>5</sub> bulk metallic glass, which was attributed to collective motion of atoms. Furthermore, the atomic volumes in the equilibrium liquid region were studied, the results can be well described by Cohen–Grest model. Meanwhile, Slipenyuk and Eckert [32] investigated the correlation between enthalpy changes and free volume reduction during structural relaxation process in this bulk metallic glass. They suggested that the low-temperature structural relaxation in Zr<sub>55</sub>Cu<sub>30</sub>Al<sub>10</sub>Ni<sub>5</sub> bulk metallic glass combined topological short range ordering (TSRO) and a chemical short range ordering (CSRO). However, to the best of our knowledge, structural relaxation in Cu<sub>46</sub>Zr<sub>45</sub>Al<sub>7</sub>Y<sub>2</sub> bulk metallic glass using differential scanning calorimetry has not yet been reported.

Based on the above analysis, in the present work, the relaxation process in Cu<sub>46</sub>Zr<sub>45</sub>Al<sub>7</sub>Y<sub>2</sub> and Zr<sub>55</sub>Cu<sub>30</sub>Ni<sub>5</sub>Al<sub>10</sub> bulk metallic glasses is studied by differential scanning calorimetry (DSC). Relevant parameters, such as heating rate, cooling rate, annealing temperature and annealing time, were considered.

In addition, an other question is open: either reversible or irreversible phenomena can occur during structural relaxation in some bulk metallic glasses, which may be due to modification of the topological range order or variation of the chemical short range order [33]. This paper addresses also this question in the two investigated bulk metallic glasses. The relevant relaxation phenomena during isothermal relaxation process are interpreted by the free volume theory or the quasi-point defect model.

## 2. Theoretical background

Enthalpy change ( $\Delta H$ ) during structural relaxation in materials could be described as follows [32,34]:

$$\Delta H = \alpha \cdot \Delta v \quad (1)$$

**Table 1**

Thermal parameters of Zr<sub>55</sub>Cu<sub>30</sub>Ni<sub>5</sub>Al<sub>10</sub> and Cu<sub>46</sub>Zr<sub>45</sub>Al<sub>7</sub>Y<sub>2</sub> bulk metallic glasses determined by DSC: glass transition temperature (*T<sub>g</sub>*), temperature of crystallization onset (*T<sub>x</sub>*), peak temperature of crystallization (*T<sub>p</sub>*), super-cooled liquid temperature ranges ( $\Delta T_x$ ,  $\Delta T = T_x - T_g$ ) and crystallization enthalpy ( $\Delta H_x$ ).

Alloys	<i>T<sub>g</sub></i> (K) ( $\pm 1$ )	<i>T<sub>x</sub></i> (K) ( $\pm 1$ )	<i>T<sub>p</sub></i> (K) ( $\pm 1$ )	$\Delta T_x$ (K)	$\Delta H_x$ (J/g) ( $\pm 2$ )
Zr-based	676	759	763	83	69.9
Cu-based	691	761	766	70	55.8

where  $\alpha$  is a constant,  $\Delta v$  is free volume or quasi-point defect concentration change during structural relaxation.

In previous publications [35,36], the Kohlrausch–Williams–Watts (KWW) equation was successfully used to describe the kinetics of the enthalpy relaxation in bulk metallic glasses, such as Pd<sub>40</sub>Cu<sub>30</sub>Ni<sub>10</sub>P<sub>20</sub> [35] or La<sub>55</sub>Al<sub>25</sub>Ni<sub>10</sub>Cu<sub>10</sub> [36]. The KWW function is defined as follows:

$$\varphi(t) = \exp \left[ - \left( \frac{t_a}{\tau} \right)^\beta \right] \quad (2)$$

where *t<sub>a</sub>* is the annealing time,  $\tau$  is the average enthalpy relaxation time,  $\beta$  is the Kohlrausch exponent whose value is between 0 and 1.

During the isochronal DSC curve process, the enthalpy relaxation is characterized by the relaxed (or recovered) enthalpy. Therefore, the recovered enthalpy ( $\Delta H(T_a)$ ) is defined as [19,34,35,37]:

$$\Delta H(T_a) = \Delta H_{eq} \left\{ 1 - \exp \left[ - (t_a/\tau)^\beta \right] \right\} \quad (3)$$

where  $\Delta H_{eq}$  is the equilibrium value of  $\Delta H_{eq}$  as *t<sub>a</sub>*  $\rightarrow$   $\infty$  at the different annealing temperatures.

It has been recognized in the literature that  $\beta$ , the Kohlrausch exponent lower than 1 reflects a broad distribution of relaxation time and not a single Debye relaxation time. For instance Hodge [38] interpreted the nonexponentiality as being a consequence of cooperativity in the motion of the rearranging structural units within the glass former. Böhmer et al. [39] reported a very interesting review on nonexponential relaxations in about 70 strong and fragile glass formers. A lot of experimental methods have been used to determine the coefficient  $\beta$ . These methods include dielectric and specific heat spectroscopy, viscoelastic modulus measurements in the shear and tensile modes as well as shear compliance investigations, quasi-elastic light scattering experiments and others. Numerous theoretical approaches have been developed to find a physical meaning to this parameter. But this is still an open question and microscopic interpretation of the stretching parameter  $\beta$  varies from one theory to another. Experimental values of  $\beta$  are in the range (0.24–1). For polymers, values extend from 0.24 (PVC) to 0.55 (polyisobutylene), for alcohols from 0.45 to 0.75, while for orientational glasses and networks values are up to 1 (for GeO<sub>2</sub>). Bulk metallic glasses appear to be in the middle of this range [5].

Concerning the average enthalpy relaxation time  $\tau$ , a lot of models have also been proposed. The simplest one uses a classical Arrhenius function:

$$\tau = \tau_0 \cdot \exp[E_a/(RT)] \quad (4)$$

where  $\tau_0$  is the pre-exponential factor, *E<sub>a</sub>* is the apparent activation energy. Relaxation times in the Zr<sub>45.0</sub>Cu<sub>39.3</sub>Al<sub>7.0</sub>Ag<sub>8.7</sub> [34] and Zr<sub>58.5</sub>Cu<sub>15.6</sub>Ni<sub>12.8</sub>Al<sub>10.3</sub>Nb<sub>2.8</sub> [40] bulk metallic glasses are in good agreement with equation (4).

Some authors [35,36,41,42] have shown that the temperature dependence of  $\tau$  was best fitted by the Vogel–Fulcher–Tamman (VFT) equation:

$$\tau = \tau_0 \cdot \exp \left( \frac{B}{T - T_0} \right) \quad (5)$$

where *B* and *T<sub>0</sub>* are temperature independent constants,  $\tau_0$  is a fitting constant.

Furthermore, the Tool–Narayanaswamy–Moynihan (TNM) model was also used to describe the enthalpy relaxation or structural relaxation in amorphous solids [9,43–48]. In this model:

$$\tau = A \cdot \exp \left[ x \frac{\Delta h^*}{RT} + \frac{(1-x)\Delta h^*}{RT_f} \right] \quad (6)$$

where  $A$  is a pre-exponential factor,  $x$  is a nonlinear parameter,  $\Delta h^*$  is the activation energy of structural relaxation in amorphous materials,  $R$  is the gas constant,  $T$  is temperature and  $T_f$  is the fictive temperature. So the question of temperature dependence of the characteristic time is still an open problem.

Finally, let us briefly recall that the quasi-point defects model is effective to describe the structural relaxation in the glassy polymers or bulk metallic glasses [5,13]. When  $T < T_g$ , the defects concentration ( $C_d$ ) in amorphous materials can be defined as follows:

$$C_d = \frac{1}{1 + \exp(\Delta S_F/R) \cdot \exp(-\Delta H_F/RT)} \quad (7)$$

where  $\Delta S_F$  and  $\Delta H_F$  are the increments of entropy and enthalpy of formation of the quasi-point defects, respectively. In this model, structural relaxation can be described according to diffusion-aided annihilation of the defects until new thermodynamic equilibrium was formed when  $T < T_g$  [13].

### 3. Experimental procedure

#### 3.1. Samples preparation

In this work,  $\text{Cu}_{46}\text{Zr}_{45}\text{Al}_7\text{Y}_2$  and  $\text{Zr}_{55}\text{Cu}_{30}\text{Ni}_5\text{Al}_{10}$  bulk metallic glasses have been kindly provided by Prof. Y. Yokoyama, Institute of Materials Research, Tohoku University, Sendai, Japan. The cylindrical samples were mechanically cut to prepare DSC samples. Prior to experiments, the samples were polished carefully using diamond paste to remove surface oxidation. Then, the samples were washed by ethanol in the ultrasonic cleaning machine.

#### 3.2. Characterization and thermal analysis

X-ray diffraction experiments in the bulk metallic glasses were conducted at room temperature to examine their amorphous character using  $\text{Cu K}\alpha$  radiation produced by a commercial device (D8, Bruker AXS GmbH, Germany). The working conditions were 40 kV and 40 mA for the X-ray tube and a scanning rate of  $0.049^\circ$  per step.

Differential scanning calorimetry (DSC) experiments were performed using a standard commercial instrument (Pekin Elmer, DSC-7) under high purity dry nitrogen at a flow rate of  $20 \text{ ml min}^{-1}$ . Aluminium pans were used as sample holders. In order to ensure the reliability of the data in the experiments, a temperature calibration was carried out prior to conducting the experiments with an indium standard specimen with 6.146 mg ( $T_g = 429.7 \text{ K}$ ,  $\Delta H_c = 28.48 \text{ J/g}$ ) and Zinc standard with 3.283 mg ( $T_g = 692.6 \text{ K}$ ,  $\Delta H_c = 108.37 \text{ J/g}$ ), which give an accuracy of  $\pm 0.2 \text{ K}$  and  $\pm 0.02 \text{ mW}$  respectively. In order to get a better accuracy during the experiments, all the samples have a similar mass, about 40 mg. Procedure used for enthalpy relaxation measurement includes two steps: first the samples were heated to the annealing temperature  $T_a$  at heating rate  $0.33 \text{ K/s}$ , held isothermally at this temperature for different times, and finally cooled down to the room temperature at  $2 \text{ K/s}$ . Then a second continuous heating was performed at  $0.33 \text{ K/s}$  in nitrogen atmosphere to detect the influence of the preliminary annealing.

### 4. Results and analysis

#### 4.1. XRD analysis of the bulk metallic glasses

The XRD patterns in the as-cast of  $\text{Cu}_{46}\text{Zr}_{45}\text{Al}_7\text{Y}_2$  and  $\text{Zr}_{55}\text{Cu}_{30}\text{Ni}_5\text{Al}_{10}$  bulk metallic glasses exhibited broad diffraction peak, the sharp diffraction peak corresponding to crystalline structure cannot be founded. So,  $\text{Cu}_{46}\text{Zr}_{45}\text{Al}_7\text{Y}_2$  and  $\text{Zr}_{55}\text{Cu}_{30}\text{Ni}_5\text{Al}_{10}$  bulk metallic glasses show the typical characteristics of an amorphous structure.

#### 4.2. Thermal properties of the bulk metallic glasses

DSC curves recorded during continuous heating at  $0.33 \text{ K/s}$  are presented in Fig. 1. DSC curves show distinct glass transition, followed by a broad super-cooled liquid region (SLR) and finally crystallization reactions at high temperature. Glass transition temperature ( $T_g$ ), temperature corresponding to the onset of crystallization ( $T_x$ ), crystallization peak temperature ( $T_p$ ) and overshoot near the glass transition ( $\Delta C_p$ ) are defined in insets (a) and (b). Values of  $T_g$ ,  $T_x$ ,  $T_p$  and super-cooled liquid temperature ranges ( $\Delta T$ ,  $\Delta T = T_x - T_g$ ) of the two bulk metallic glass are given in Table 1. Present results are in good agreement with previously reported ones [37,45,49–51].

Fig. 2 shows DSC curves (with different scales) in  $\text{Cu}_{46}\text{Zr}_{45}\text{Al}_7\text{Y}_2$  and  $\text{Zr}_{55}\text{Cu}_{30}\text{Ni}_5\text{Al}_{10}$  bulk metallic glasses with different heating rates. The relevant thermal parameters shift to higher temperatures by increasing the heating rate, indicating clearly the kinetics aspects of both glass transition and crystallization processes.

The activation energy  $E_a$  of phase transformation occurring in bulk metallic glass is usually determined using DSC experiments carried out with various heating rates and then calculated using the Kissinger's formula [50–52]:

$$\ln(R_h/T_p^2) = -\frac{E_a}{RT_p} + C \quad (8)$$

where  $R_h$  is the heating rate,  $R$  is the gas constant and  $C$  is a constant. Fig. 3(a) shows the variation of  $\ln(R_h/T_p^2)$  versus ( $1000/T_p$ ) in  $\text{Cu}_{46}\text{Zr}_{45}\text{Al}_7\text{Y}_2$  and  $\text{Zr}_{55}\text{Cu}_{30}\text{Ni}_5\text{Al}_{10}$  bulk metallic glasses. The activation energy for crystallization progress is  $3.18 \text{ eV}$  in  $\text{Cu}_{46}\text{Zr}_{45}\text{Al}_7\text{Y}_2$ , and  $3.19 \text{ eV}$  in  $\text{Zr}_{55}\text{Cu}_{30}\text{Ni}_5\text{Al}_{10}$ , respectively. These values are fairly similar.

In addition, the Flynn–Wall–Ozawa method is another widely used method to calculate the apparent activation energy for bulk metallic glasses during the non-isothermal crystallization process [53]. The apparent activation energy was evaluated by the following equation:

$$\ln(R_h) = -1.052 \frac{E_a}{RT_p} + C \quad (9)$$

Fig. 3(b) presents the variation of  $\ln(R_h)$  with  $1000/T_p$  in  $\text{Cu}_{46}\text{Zr}_{45}\text{Al}_7\text{Y}_2$  and  $\text{Zr}_{55}\text{Cu}_{30}\text{Ni}_5\text{Al}_{10}$  bulk metallic glasses. The

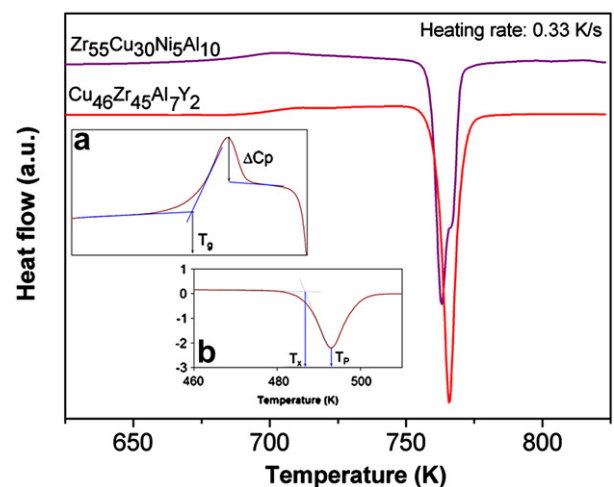
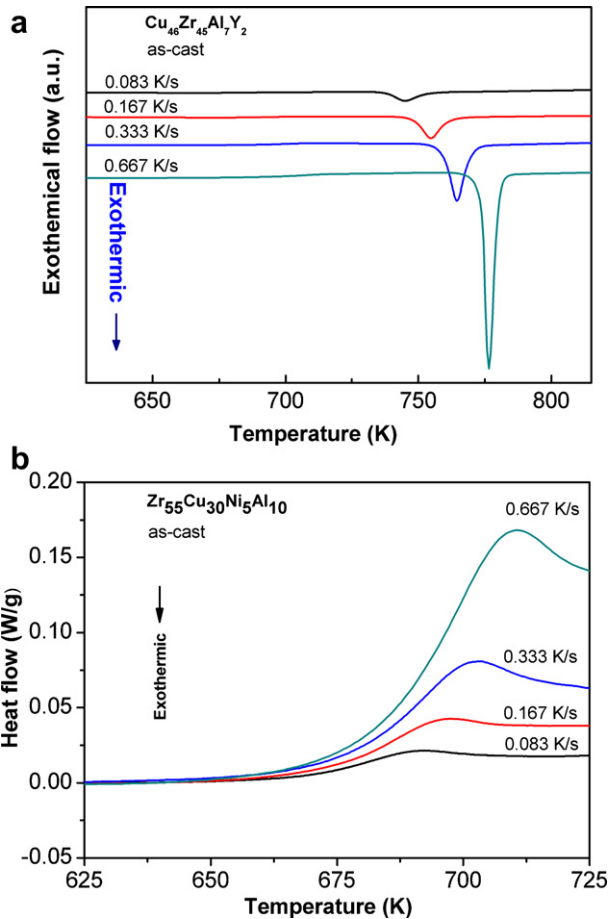


Fig. 1. DSC curves in  $\text{Zr}_{55}\text{Cu}_{30}\text{Ni}_5\text{Al}_{10}$  and  $\text{Cu}_{46}\text{Zr}_{45}\text{Al}_7\text{Y}_2$  bulk metallic glasses at a heating rate of  $0.33 \text{ K/s}$ .  $T_g$ ,  $T_x$ ,  $T_p$  and glass transition peak height ( $\Delta C_p$ ) are defined in insets (a) and (b).



**Fig. 2.** Isochronal DSC curves in  $\text{Cu}_{46}\text{Zr}_{45}\text{Al}_7\text{Y}_2$  (a) and  $\text{Zr}_{55}\text{Cu}_{30}\text{Ni}_5\text{Al}_{10}$  (b) bulk metallic glasses.  $T_g$ ,  $T_x$ ,  $T_p$  in the two bulk metallic glasses shift to higher temperature with increasing heating rate.

activation energies of crystallization in  $\text{Cu}_{46}\text{Zr}_{45}\text{Al}_7\text{Y}_2$  and  $\text{Zr}_{55}\text{Cu}_{30}\text{Ni}_5\text{Al}_{10}$  bulk metallic glasses are 3.16 eV and 3.18 eV, respectively. These results are consistent with the Flynn–Wall–Ozawa equation and Kissinger's formula. The explanation is fairly simple: since the variation of  $R_h$  is much larger than that of  $T_p$ , the two formulas give automatically the same result.

So, these alloys have a good resistance to crystallization, compared to other BMG. Indeed, these values are higher than those reported in other amorphous alloys: 2.3 eV in  $\text{Cu}_{50}\text{Zr}_{50}$  [54], 1 eV in  $\text{Mg}_{58.5}\text{Cu}_{30}\text{Dy}_{11.5}$  [55] and 2.37 eV in  $\text{Pd}_{40}\text{Ni}_{10}\text{Cu}_{30}\text{P}_{20}$  [55].

#### 4.3. Kinetic fragility

According to Angell's suggestion [56,58,59], glasses could be classified into two groups, namely, strong glasses and fragile glasses, depending on the value of the fragility index ( $m$ ) defined as:

$$m = \left. \frac{d \log \tau}{d(T_g/T)} \right|_{T=T_g} = \frac{E_g}{RT_g \ln 10} \quad (10)$$

where  $\tau$  is the characteristic relaxation time at the glass transition temperature  $T_g$  and  $E_g$  is the activation energy for glass transition. A large value of  $m$  corresponds to a fragile amorphous material with a large deviation from the Arrhenius law [39]. The fragility index can be related to the shear viscosity  $\eta$  [39,60,61]:

$$m = \left. \frac{d \log \eta(T)}{d(T_g/T)} \right|_{T=T_g} \quad (11)$$

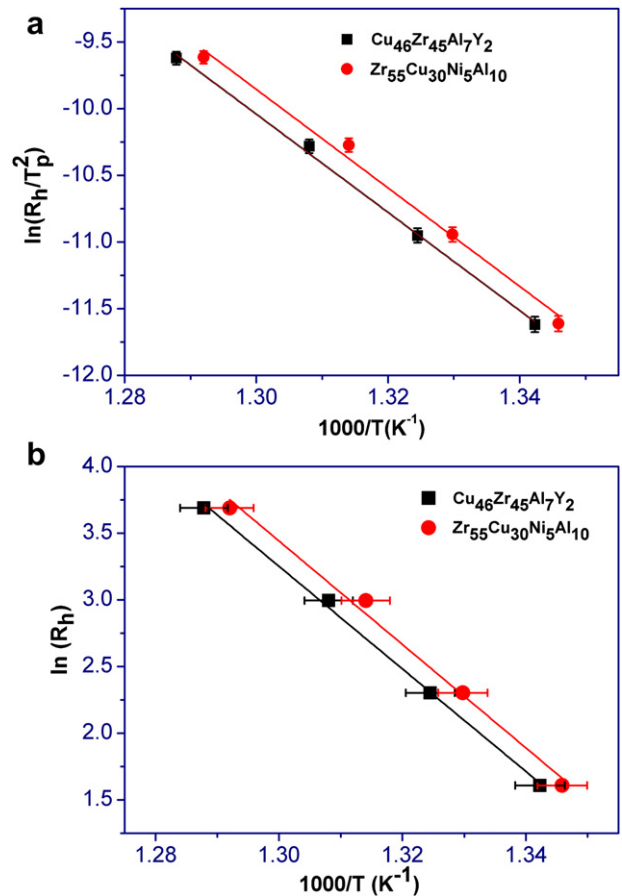


**Fig. 3.** (a) Kissinger plots for  $\text{Cu}_{46}\text{Zr}_{45}\text{Al}_7\text{Y}_2$  and  $\text{Zr}_{55}\text{Cu}_{30}\text{Ni}_5\text{Al}_{10}$  bulk metallic glasses; (b) Flynn–Wall–Ozama plots for  $\text{Cu}_{46}\text{Zr}_{45}\text{Al}_7\text{Y}_2$  and  $\text{Zr}_{55}\text{Cu}_{30}\text{Ni}_5\text{Al}_{10}$  bulk metallic glasses. Solid lines correspond to a linear function fitting the experimental data.

Or to the dependence of  $T_g$  on the heating rate  $R_h$ , assuming a Vogel–Fulcher–Tamman (VFT) relation [36,41,52]:

$$m = \frac{D^* T_g^0}{\ln 10 (T_g - T_g^0)^2} \quad (12)$$

where  $A$ ,  $D^*$  and  $T_g^0$  are fitting parameters.

In the present work, dynamics kinetic fragility parameter  $m$  was calculated by equation (10) at the heating rate of 0.33 K/s. Thus, the kinetic fragility parameters  $m$  in  $\text{Cu}_{46}\text{Zr}_{45}\text{Al}_7\text{Y}_2$  and  $\text{Zr}_{55}\text{Cu}_{30}\text{Ni}_5\text{Al}_{10}$  bulk metallic glasses are 72 and 69, respectively. It is interesting to note also that compared with  $\text{Zr}_{41.2}\text{Ti}_{13.8}\text{Cu}_{12.5}\text{Ni}_{10}\text{Be}_{22.5}$  ( $m = 59$ ) [62],  $\text{Zr}_{46.75}\text{Ti}_{8.25}\text{Cu}_{7.5}\text{Ni}_{10}\text{Be}_{27.5}$  ( $m = 44.2$ ) [63],  $\text{Zr}_{55}\text{Al}_{22.5}\text{Co}_{22.5}$  ( $m = 73$ ) [64] and  $\text{Zr}_{11}\text{Ti}_{34}\text{Cu}_{47}\text{Ni}_8$  ( $m = 68$ ) [64],  $\text{Zr}_{55}\text{Cu}_{30}\text{Ni}_5\text{Al}_{10}$  bulk metallic glass exhibited a value of  $m$  similar to that reported in other Zr-based bulk metallic glasses, implying that  $\text{Zr}_{55}\text{Cu}_{30}\text{Ni}_5\text{Al}_{10}$  bulk metallic glass has also an intermediate behaviour. A similar conclusion can be obtained in the  $\text{Cu}_{46}\text{Zr}_{45}\text{Al}_7\text{Y}_2$  bulk metallic glass, since the value of  $m$  is also similar to those reported on other Cu-based BMG, such as  $\text{Cu}_{47}\text{Ti}_{34}\text{Zr}_{11}\text{Ni}_8$  ( $m = 68$ ) [62] and  $\text{Cu}_{43}\text{Zr}_{43}\text{Al}_7\text{Be}_7$  ( $m = 43$ ) [57].

#### 4.4. Annealing experiments in the bulk metallic glasses

To analyze effects of the annealing temperature on enthalpy relaxation, bulk metallic glasses were annealed at different temperatures in pure nitrogen atmosphere, then cooled down to 573 K and finally heated up to 823 K. In the Cu-based bulk metallic glass, three

annealing temperatures have been retained, below  $T_g$ :  $T_a = 664$  and  $674$  K. In Zr-based bulk metallic glass, the following temperatures have been chosen:  $644$ ,  $649$ ,  $659$ ,  $669$  and  $674$  K. Fig. 4 presents selected final DSC curves carried out with a heating rate of  $0.33$  K/s, after different annealing times. Overshoots are always observed near the glass transition temperature, during the heating performed after the annealing.

Therefore, the enthalpy relaxation process is significantly sensitive to annealing time and annealing temperature. The final magnitude decreases when the annealing temperature increases, while the kinetics is accelerated by an increase in annealing temperature. These results are in agreement with that reported by other research groups [31,34,35,40].

#### 4.4.1. Analysis of the effect of annealing time (at a given annealing temperature $T_a$ )

The recovery enthalpy of the bulk metallic glasses, calculated from DSC curves, can be well fitted by the equation (3) (Fig. 5). The Kohlrausch exponent  $\beta$  and the enthalpy relaxation time  $\tau$  are listed in Table 2 (results reported in previous publications in other bulk metallic glasses have been added) (The relationship between enthalpy relaxation time and annealing temperature for Zr-based bulk metallic glass is shown in Fig. 6). In the previous investigations, values of  $\beta$  determined in the  $Zr_{58.5}Cu_{15.6}Ni_{12.8}Al_{10.3}Nb_{2.8}$  bulk metallic glass increased with increasing the annealing temperature  $T_a$  [34]. In contrast, the value of  $\beta$  in the  $La_{55}Al_{25}Ni_{10}Cu_{10}$  bulk metallic glass was constant, around  $0.78$  [35]. In the present work,  $\beta$  values in  $Zr_{55}Cu_{30}Ni_5Al_{10}$  bulk metallic glass range from  $0.69$  to  $0.78$ ,  $\beta$  values in the  $Cu_{46}Zr_{45}Al_7Y_2$  bulk metallic glass are  $0.62$  ( $T_a = 674$  K) and  $0.68$  ( $T_a = 664$  K), respectively. These values are in good agreement with that reported by Böhmer et al. [39], who indicated that these values in bulk metallic glasses are intermediate between those found in polymers and those corresponding to oxide

glasses. Furthermore an increase of  $\beta$  with the temperature appears logical. Indeed, it has been recognized in the literature that  $\beta$ , the Kohlrausch exponent lower than  $1$ , reflects a broad distribution of relaxation time and not a single Debye relaxation time. When the temperature increases the atomic mobility is easier, the distribution width of relaxation time decreases and consequently,  $\beta$  approaches  $1$ .

Fig. 7 illustrates the relationship between the characteristic time  $\tau$  and the annealing temperature  $T_a$  in  $Zr_{55}Cu_{30}Ni_5Al_{10}$  bulk metallic glass. As for any thermally assisted phenomenon, the first solution to be tested is an Arrhenius law (equation (4)). This assumption is valid, since a linear dependence is observed between  $\ln(\tau)$  and  $(1/T)$ . The apparent activation energy is  $5.44$  eV and the pre-exponential time is about  $10^{-39}$  s. These values appear unrealistic for a simple process. Indeed, in this case  $\tau$  should be close to the elementary Debye characteristic time ( $10^{-12}$ – $10^{-13}$  s) and  $E_a$  should be in the range  $1$ – $2$  eV. Therefore the only solution is the existence of correlated movements. The hierarchical correlation concept introduced by Palmer et al. was developed by Perez [14–16] and linked to the movements of atoms (or molecules) assisted by quasi-point defects. In this model, the global characteristic time  $\tau_{mol}$ , was given by:

$$\tau_{mol} = t_0 \left( \frac{\tau_\beta}{t_0} \right)^{1/\chi} \quad (13)$$

$\tau_{mol}$  corresponds to the mean duration of the movement of a structural unit over a distance equal to its dimension.  $\tau_\beta$  is the mean time of the thermally activated jump of a structural unit and follows an Arrhenius law:

$$\tau_\beta = \tau_0 \cdot \exp\left(\frac{E_a}{kT}\right) \quad (14)$$

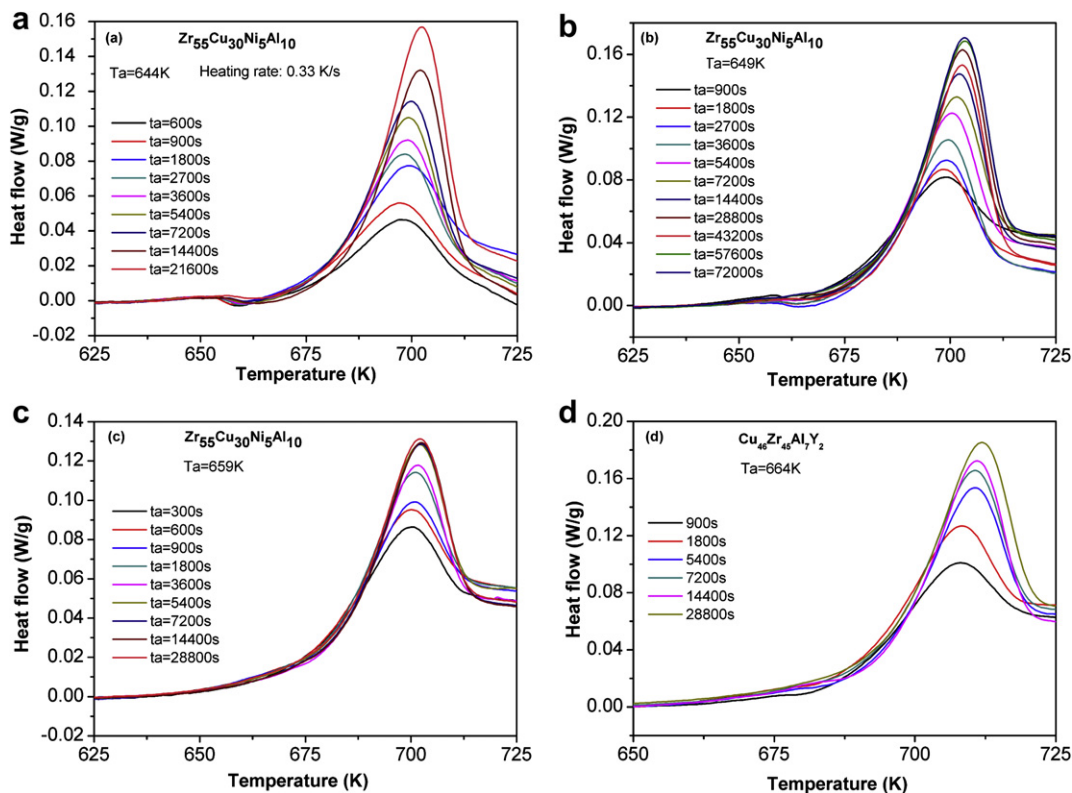


Fig. 4. Recovery enthalpy measurements in  $Zr_{55}Cu_{30}Ni_5Al_{10}$  and  $Cu_{46}Zr_{45}Al_7Y_2$  bulk metallic glasses after different annealing times at a heating rate of  $0.33$  K/s. (a)  $Zr_{55}Cu_{30}Ni_5Al_{10}$  annealed at  $644$  K; (b)  $Zr_{55}Cu_{30}Ni_5Al_{10}$  annealed at  $649$  K; (c)  $Zr_{55}Cu_{30}Ni_5Al_{10}$  annealed at  $659$  K; (d)  $Cu_{46}Zr_{45}Al_7Y_2$  annealed at  $664$  K.

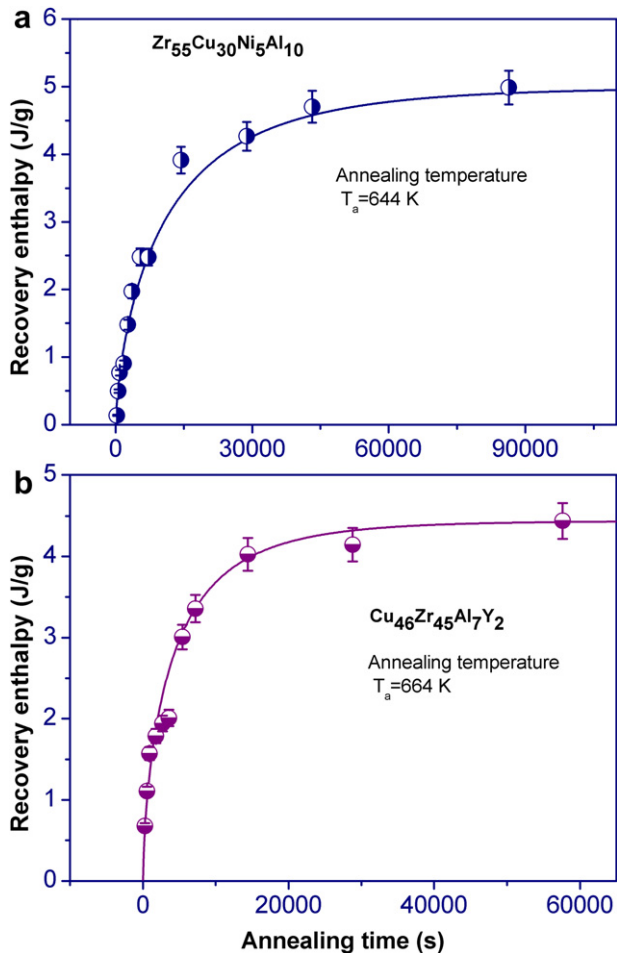


Fig. 5. Values of recovery enthalpy of  $Zr_{55}Cu_{30}Ni_5Al_{10}$  and  $Cu_{46}Zr_{45}Al_7Y_2$  bulk metallic glasses calculated from DSC curves and fitted by equation (3) (solid line). (a)  $Zr_{55}Cu_{30}Ni_5Al_{10}$  annealed at 644 K; (b)  $Cu_{46}Zr_{45}Al_7Y_2$  annealed at 664 K.

where  $E_a$  is the activation energy for the structural unit movement,  $t_0$  is a scaling factor and  $\chi$  is a correlation factor, ranging from 0 (full order) to 1 (full disorder).  $\chi$  is linked to the quasi-point defect concentration. Below  $T_g$ , i.e. in an isoconfigurational state,  $\chi$  is constant. Consequently a plot of  $\ln(\tau_{mol})$  versus the reciprocal of the temperature should also give a straight line, but the slope is not related to  $E_a$ , but to  $E_a/\chi$ . And since  $\chi$  is typically 0.3–0.4 in bulk metallic glasses [17], the effective activation energy is not 5.44 eV, but in the range 1.5–2 eV. In addition, the effective characteristic time is much higher than  $10^{-39}$  s. In conclusion, these values can be interpreted in a realistic way using this physical model based on the concept of quasi-point defect. Finally, let us mention that the VFT law (equation (5)) is usually applied only above  $T_g$ , where  $\chi$  is then temperature dependent and so equation (9) is more complex to use to determine  $E_a$  and  $\tau_{mol}$ .

Annealing time has little effect on  $T_g$ ,  $T_x$  and  $T_p$  in the two bulk metallic glasses (Fig. 8(a), (b)). However, when the annealing time is long enough,  $T_g$  increases while  $T_x$  is decreasing. Wang et al. [49] studied the structural relaxation in  $Pd_{40}Cu_{30}Ni_{10}Pd_{20}$  bulk metallic glass and proposed that this evolution observed when the annealing time is too long is due to new defects on the interfaces between the solid–liquid regions in the bulk metallic glass. Wang et al. [45] proposed that in such conditions partial decomposition has occurred in the residual amorphous matrix. In other words, compared with as-cast alloys, crystallization nuclei may be created during a long annealing time. These assumptions are fairly difficult

Table 2  
Kohlrausch exponents ( $\beta$ ) and relaxation time  $\tau$  of the bulk metallic glasses (present work and previous literatures).

Metallic glasses	$T_a$ (K)	$\tau$ (s)	$\beta$	References
$Cu_{46}Zr_{45}Al_7Y_2$	674	1011	0.68 ( $\pm 0.05$ )	Present work
$Cu_{46}Zr_{45}Al_7Y_2$	664	4323	0.62 ( $\pm 0.04$ )	Present work
$Zr_{55}Cu_{30}Ni_5Al_{10}$	674	143	–	Present work
$Zr_{55}Cu_{30}Ni_5Al_{10}$	669	380	0.79 ( $\pm 0.04$ )	Present work
$Zr_{55}Cu_{30}Ni_5Al_{10}$	659	1460	0.78 ( $\pm 0.04$ )	Present work
$Zr_{55}Cu_{30}Ni_5Al_{10}$	649	6300	0.69 ( $\pm 0.05$ )	Present work
$Zr_{55}Cu_{30}Ni_5Al_{10}$	644	12,000	0.71 ( $\pm 0.05$ )	Present work
$Zr_{58.5}Cu_{15.6}Ni_{12.8}Al_{10.3}Nb_{2.8}$	633		0.79	[40]
$Zr_{58.5}Cu_{15.6}Ni_{12.8}Al_{10.3}Nb_{2.8}$	643		0.80	[40]
$Zr_{58.5}Cu_{15.6}Ni_{12.8}Al_{10.3}Nb_{2.8}$	653		0.89	[40]
$Zr_{58.5}Cu_{15.6}Ni_{12.8}Al_{10.3}Nb_{2.8}$	663		0.86	[40]
$Zr_{45.0}Cu_{39.3}Al_{7.0}Ag_{8.7}$	648	2643.5	0.717	[34]
$Zr_{45.0}Cu_{39.3}Al_{7.0}Ag_{8.7}$	658	1584.4	0.749	[34]
$Zr_{45.0}Cu_{39.3}Al_{7.0}Ag_{8.7}$	668	1047.5	0.825	[34]
$Zr_{45.0}Cu_{39.3}Al_{7.0}Ag_{8.7}$	678	497.7	0.843	[34]
$Zr_{45.0}Cu_{39.3}Al_{7.0}Ag_{8.7}$	684	242.8	0.892	[34]
$La_{55}Al_{25}Ni_{10}Cu_{10}$	445	2503	0.77	[35]
$La_{55}Al_{25}Ni_{10}Cu_{10}$	435	3597	0.79	[35]
$La_{55}Al_{25}Ni_{10}Cu_{10}$	425	5447	0.78	[35]
$La_{55}Al_{25}Ni_{10}Cu_{10}$	415	8199	0.77	[35]
$Zr_{55}Cu_{30}Al_{10}Ni_5$	623	123,195	0.35	[37]
$Zr_{55}Cu_{30}Al_{10}Ni_5$	633	48,901	0.39	[37]
$Zr_{55}Cu_{30}Al_{10}Ni_5$	643	13,888	0.59	[37]
$Zr_{55}Cu_{30}Al_{10}Ni_5$	653	2352	0.69	[37]
$Zr_{55}Cu_{30}Al_{10}Ni_5$	660	1430	0.65	[37]
$Pd_{42.5}Cu_{30}Ni_{7.5}P_{20}$	549	3269	0.52	[19]
$Pd_{40}Ni_{40}P_{20}$	549	1840	0.66	[19]
$Zr_{62}Al_8Ni_{13}Cu_{17}$	703–3 min	1514	0.61	[45]
$Zr_{62}Al_8Ni_{13}Cu_{17}$	703–5 min	586	0.84	[45]
$Pd_{43}Ni_{10}Cu_{27}P_{20}$	557	2237.4	0.7	[60]
$Pd_{43}Ni_{10}Cu_{27}P_{20}$	561	1262.9	0.68	[60]
$Pd_{43}Ni_{10}Cu_{27}P_{20}$	565	698.3	0.69	[60]
$Pd_{43}Ni_{10}Cu_{27}P_{20}$	569	395.5	0.75	[60]
$Zr_{41.2}Ti_{13.5}Cu_{12.5}Ni_{10.0}Be_{22.5}$	573		0.61	[5]
$La_{50}Al_{25}Ni_{25}$	473	1800		[65]

to check. Indeed, the sizes the nuclei (if they really exist) are probably too small to be detected, for instance, by X-Ray diffraction. However, it appears like a realistic assumption.

Meanwhile, it can be seen from Fig. 8(c) that  $\Delta C_p$  increases with increasing the annealing time in  $Cu_{46}Zr_{45}Al_7Y_2$  and  $Zr_{55}Cu_{30}Ni_5Al_{10}$  bulk metallic glasses and then tend to equilibrium. This phenomenon corresponds to a progressive evolution of the free volume or of the quasi-point defect concentration towards the equilibrium

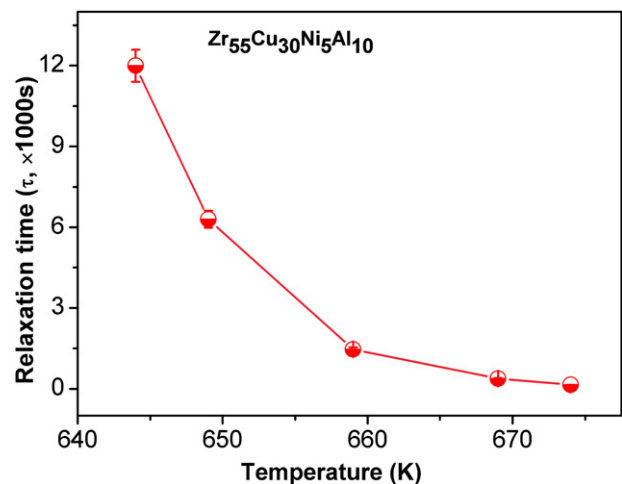


Fig. 6. Relationship between enthalpy relaxation time and annealing temperature in  $Zr_{55}Cu_{30}Ni_5Al_{10}$  bulk metallic glass.

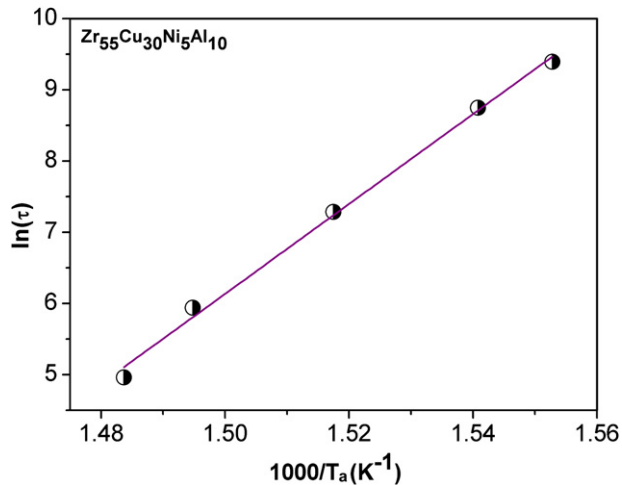


Fig. 7. Relationship between  $\ln \tau$  and reciprocal of annealing temperature  $T_a$  in  $\text{Zr}_{55}\text{Cu}_{30}\text{Ni}_5\text{Al}_{10}$  bulk metallic glass.

value corresponding to the temperature at which the annealing was conducted [38].

Furthermore, in order to analyze the effect of the annealing temperature on the crystallization peak temperature ( $T_p$ ), the relationship between the annealing time and the crystallization peak temperature ( $T_p$ ) is shown in Fig. 9. The slope of the fitting lines increases when the annealing temperature is increased, in both investigated alloys, probably due to an increase in the atomic mobility when the temperature increases.

#### 4.4.2. Analysis of the effect of annealing temperature (at a given annealing time $t_a$ )

For a given annealing time  $t_a$ , the annealing temperature  $T_a$  has a direct effect on the enthalpy relaxation in the bulk metallic glasses. Therefore, the recovery enthalpy phenomena with different  $T_a$  at given  $t_a$  in  $\text{Zr}_{55}\text{Cu}_{30}\text{Ni}_5\text{Al}_{10}$  and  $\text{Cu}_{46}\text{Zr}_{45}\text{Al}_7\text{Y}_2$  bulk metallic glasses are shown in Fig. 10. Five different  $T_a$  were used in  $\text{Zr}_{55}\text{Cu}_{30}\text{Ni}_5\text{Al}_{10}$ : 644, 649, 659, 669 and 674 K, respectively, with  $t_a = 7200$  s. Six different  $T_a$  were used in  $\text{Cu}_{46}\text{Zr}_{45}\text{Al}_7\text{Y}_2$ : 633, 643, 653, 663, 673 and 683 K, respectively, with  $t_a = 3600$  s.

It is worth noting that by increasing annealing temperature, value of recovery enthalpy in the bulk metallic glasses reaches a maximum, due to two opposite factors: when temperature increases the kinetics is accelerated, but the final magnitude is decreased and hence a maximum is observed. Position of this maximum depends on the annealing time: an increase of the annealing time should shift the maximum towards lower temperatures. A similar enthalpy relaxation behaviour has been reported in  $\text{La}_{50}\text{Al}_{25}\text{Ni}_{25}$  bulk metallic glass [65]. The physical reason is fairly simple: the difference of free volume or of concentration in quasi-point defects between the equilibrium state and the as-cast initial state decreases when approaching  $T_g$ . In addition, in the quasi-point defect model, a distribution of relaxation times is introduced and, according to this model, when annealing process proceeds at lower temperature, for example for annealing temperature  $T_a$  at 644 K for  $\text{Zr}_{55}\text{Cu}_{30}\text{Ni}_5\text{Al}_{10}$  and  $T_a$  at 633 K for  $\text{Cu}_{46}\text{Zr}_{45}\text{Al}_7\text{Y}_2$ , the less-mobile defects have a very slow kinetics and the real equilibrium is really difficult to achieve [13].

#### 4.5. Effect of the cooling rate on enthalpy relaxation

As shown in the previous section, the recovery relaxation processes in the  $\text{Zr}_{55}\text{Cu}_{30}\text{Ni}_5\text{Al}_{10}$  and  $\text{Cu}_{46}\text{Zr}_{45}\text{Al}_7\text{Y}_2$  bulk metallic

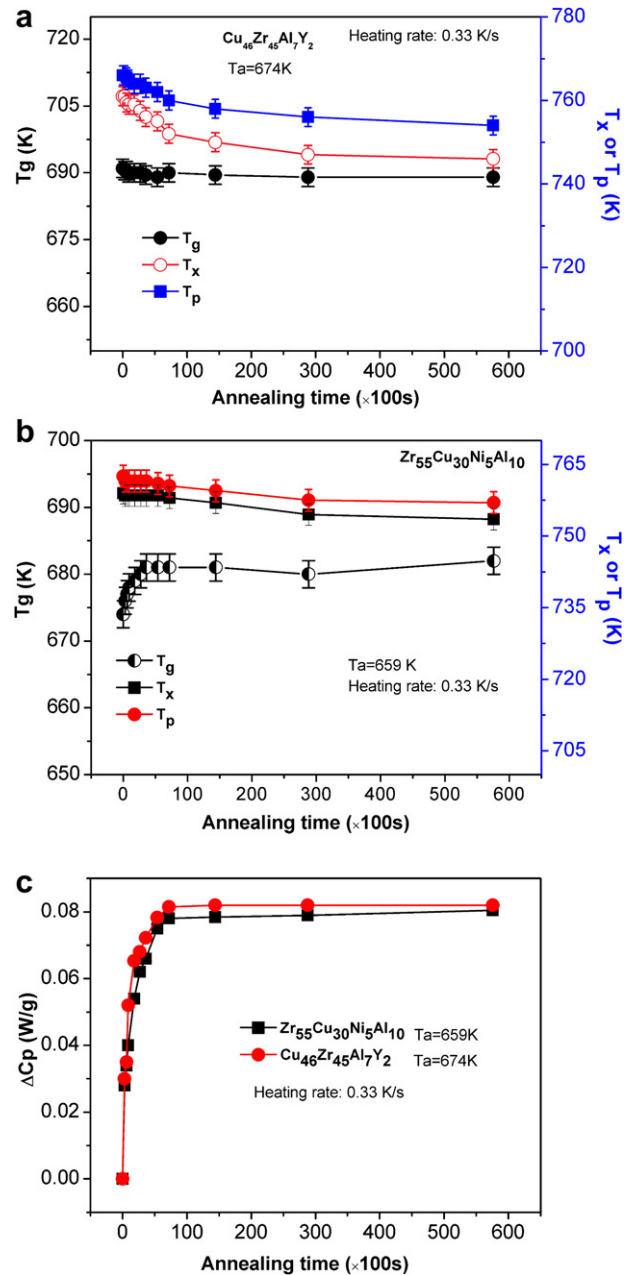
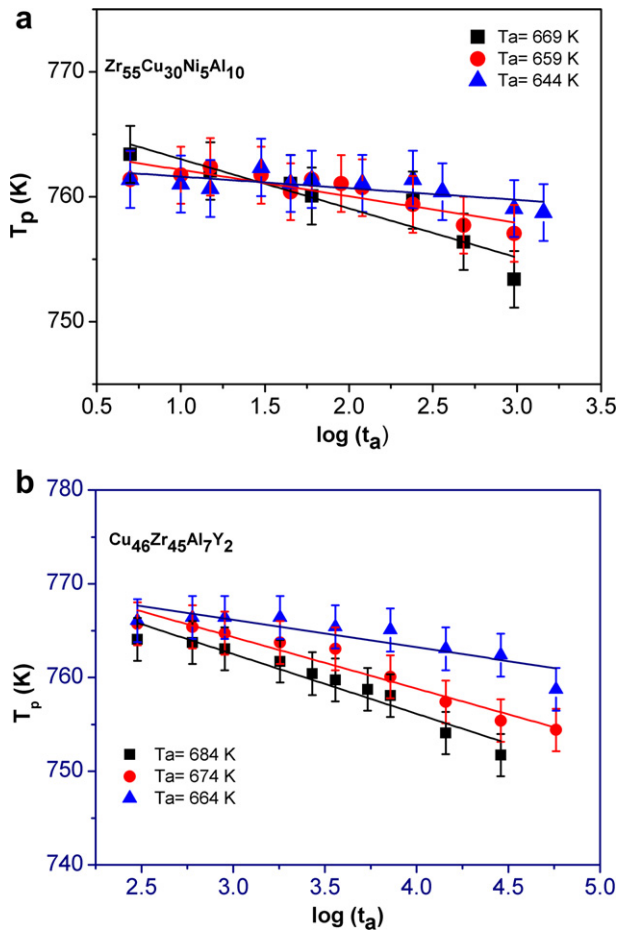


Fig. 8. Thermal parameters:  $T_g$ ,  $T_x$ ,  $T_p$ , in  $\text{Zr}_{55}\text{Cu}_{30}\text{Ni}_5\text{Al}_{10}$  and  $\text{Cu}_{46}\text{Zr}_{45}\text{Al}_7\text{Y}_2$  bulk metallic glasses. (a)  $T_g$ ,  $T_x$ ,  $T_p$  in  $\text{Cu}_{46}\text{Zr}_{45}\text{Al}_7\text{Y}_2$  annealed at 674 K after various annealing time  $t_a$ ; (b)  $T_g$ ,  $T_x$ ,  $T_p$  in  $\text{Zr}_{55}\text{Cu}_{30}\text{Ni}_5\text{Al}_{10}$  annealed at 659 K during various annealing time  $t_a$ ; (c) glass transition peak height ( $\Delta C_p$ ) in the bulk metallic glasses with different annealing times.

glasses depend both on the annealing time and on the annealing temperature for a given as-cast state. But the question is as follows: is there any effect of the initial state before annealing on this relaxation process? This initial state, characterized for instance by a given concentration of quasi-point defects, which can be modified by changing the cooling rate from a temperature above  $T_g$  to room temperature. In order to assess the question, a series of experiments with different cooling rates have been conducted using DSC. The schematic drawing of the procedures of the cooling treatment in  $\text{Cu}_{46}\text{Zr}_{45}\text{Al}_7\text{Y}_2$  bulk metallic glass is shown in Fig. 11(a), the cooling rates in the present work are 0.083, 0.167, 0.333 and 0.667 K/s, respectively. The recovery enthalpy obtained by the different cooling rates in the  $\text{Cu}_{46}\text{Zr}_{45}\text{Al}_7\text{Y}_2$  bulk metallic glass is



**Fig. 9.** Relationship between the annealing time ( $\log(t_a)$ ) and the crystallization peak temperature ( $T_p$ ) at various annealing temperatures in  $Zr_{55}Cu_{30}Ni_5Al_{10}$  and  $Cu_{46}Zr_{45}Al_7Y_2$  bulk metallic glasses: (a) Plots of  $T_p$  versus  $\log(t_a)$  in  $Zr_{55}Cu_{30}Ni_5Al_{10}$  bulk metallic glass:  $T_a = 644$ ,  $659$  and  $669$  K, respectively; (b) Plots of  $T_p$  versus  $\log(t_a)$  in  $Cu_{46}Zr_{45}Al_7Y_2$  bulk metallic glass:  $T_a = 664$ ,  $674$  and  $684$  K, respectively. Solid lines correspond to a linear function fitting the experimental data.

shown in Fig. 11(b). Similar experiments have been conducted in the  $Zr_{55}Cu_{30}Ni_5Al_{10}$  bulk metallic glass (Fig. 12).

The recovery enthalpies of the two bulk metallic glasses are independent of the cooling rates and consequently independent of

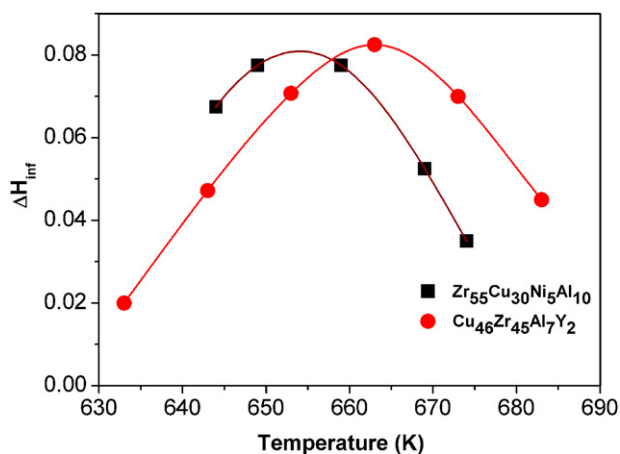


**Fig. 10.** Enthalpy relaxation in  $Zr_{55}Cu_{30}Ni_5Al_{10}$  and  $Cu_{46}Zr_{45}Al_7Y_2$  bulk metallic glasses after annealing at different temperatures: (a)  $Zr_{55}Cu_{30}Ni_5Al_{10}$ ; (b)  $Cu_{46}Zr_{45}Al_7Y_2$ .

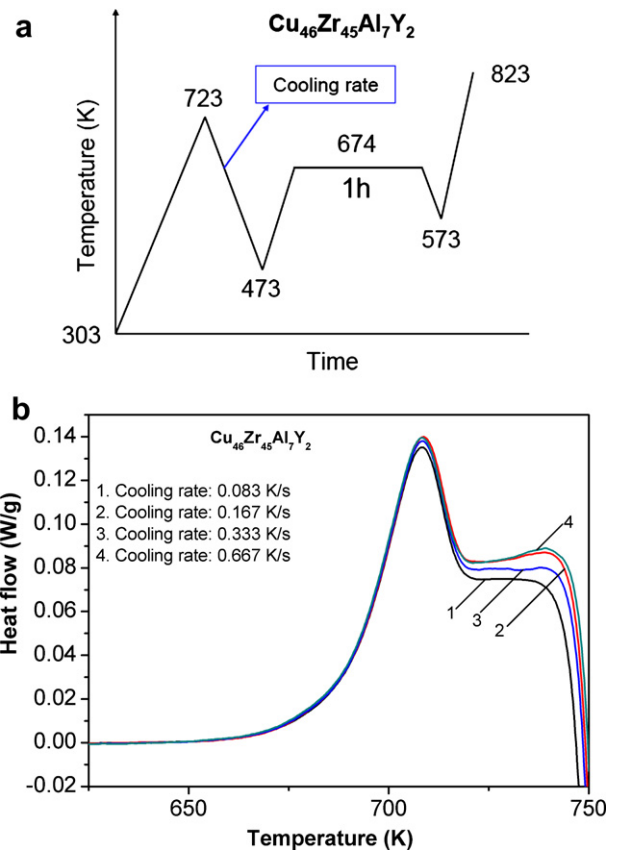


**Fig. 11.** Enthalpy relaxation behaviour of  $Cu_{46}Zr_{45}Al_7Y_2$  with various cooling rates. (a) Scheme of the thermal history; (b) Enthalpy relaxation in the  $Cu_{46}Zr_{45}Al_7Y_2$  bulk metallic glass.

the initial state before annealing. So, structural relaxation occurring during annealing erases the differences which could result from quenching performed in different conditions.

#### 4.6. Effect of heating treatment process on reversibility of the enthalpy relaxation process

As mentioned in the introduction, annealing below  $T_g$  induces the movement of atoms, in order to decrease the Gibbs energy. These atomic movements can induce both a topological short range ordering (TSRO) and a chemical short range ordering (CSRO). These phenomena have been for instance investigated in the Vit1 bulk metallic glass [33], using thermoelectric power measurement, a technique which is very sensitive to any structural evolution. TSRO is connected to a decrease of the defect concentration and is mainly reversible when the specimen is reheated above  $T_g$ , while the evolution associated to CSRO is mainly irreversible. In order to determine the reversibility of the phenomena occurring during the enthalpy relaxation process, specific heat treatments have been carried out, as illustrated in Fig. 13(a). The first annealing leads to a structural relaxation, the effect of which is observed during the subsequent heating. This heating up to a temperature higher than  $T_g$  is followed by a quenching to low temperature and finally a second heating is performed. Results are shown in Fig. 13(b) (the curve relative to a standard as-cast state has been added for comparison). The overshoot induced by annealing during 3600 s at 674 K has been nearly erased by the heating above  $T_g$  and the curve is then very similar to that corresponding to an initial un-annealed specimen. It may therefore be concluded that the enthalpy



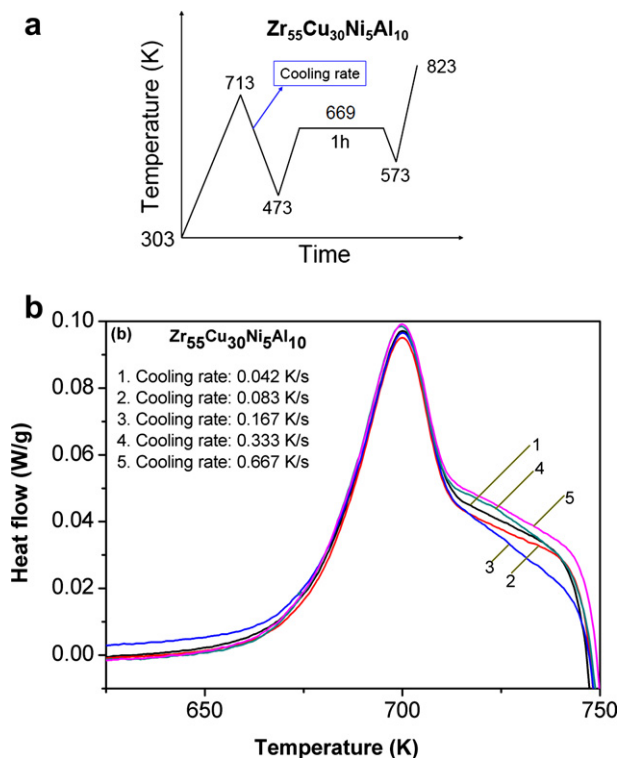


Fig. 12. Enthalpy relaxation behaviour of  $Zr_{55}Cu_{30}Ni_5Al_{10}$  with various cooling rates. (a) Scheme of the thermal history; (b) Enthalpy relaxation in the  $Zr_{55}Cu_{30}Ni_5Al_{10}$  bulk metallic glass.

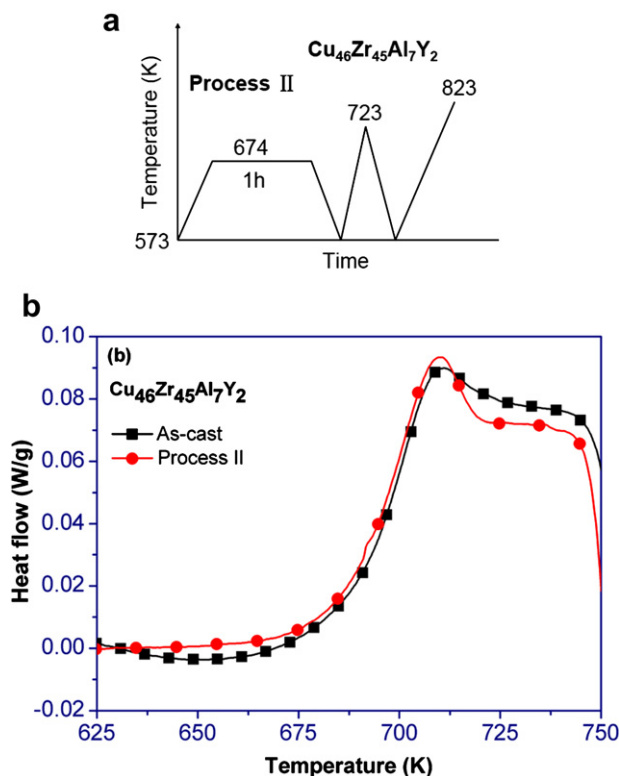


Fig. 13. Enthalpy relaxation in  $Cu_{46}Zr_{45}Al_7Y_2$  bulk metallic glass. (a) Scheme of the thermal history. (b) Results.

relaxation occurring during annealing below  $T_g$  is mainly reversible. Let us mention that if irreversible phenomena occur the crystallization phenomenon taking place at higher temperature could be affected. Similar results (not presented here) have been obtained in the Zr-based bulk metallic glass.

## 5. Conclusion

The enthalpy relaxation process and the relevant kinetic behaviour in  $Zr_{55}Cu_{30}Ni_5Al_{10}$  and  $Cu_{46}Zr_{45}Al_7Y_2$  bulk metallic glasses were investigated by DSC. Main results are as follows:

- Initial state before annealing has little effect on the enthalpy relaxation in the bulk metallic glasses
- Structural relaxation is sensitive to annealing time and annealing temperature.
- During heating after an annealing below  $T_g$ , an overshoot in specific heat is observed in the glass transition range. Its magnitude  $\Delta C_p$  characterizes the relaxation process. Its value increases with the annealing time up to a saturation value, the value of which decreases when the annealing temperature increases.
- Phenomena observed during the structural relaxation in bulk metallic glasses are mainly reversible.
- Kinetic fragility parameters  $m$  in  $Cu_{46}Zr_{45}Al_7Y_2$  and  $Zr_{55}Cu_{30}Ni_5Al_{10}$  bulk metallic glasses are 72 and 69, respectively. These two bulk metallic glasses have therefore an intermediate behaviour, similar to that of many other bulk metallic glasses.
- Enthalpy relaxation kinetics can be well fitted by a stretched exponential relaxation function. Relaxation time decreases with increasing annealing temperature, in good agreement with previously reported data in other based bulk metallic glasses.
- Structural relaxation mechanism in the bulk metallic glasses may be described by the quasi-point defects model.
- According to the Kissinger's formula, activation energy for crystallization progress is 3.18 eV in  $Cu_{46}Zr_{45}Al_7Y_2$ , and 3.19 eV in  $Zr_{55}Cu_{30}Ni_5Al_{10}$ , respectively.

## Acknowledgement

Authors wish to express their thanks to Mr. J.M. Chenal, for valuable discussion during the course of the work and Prof. Y. Yokoyama for providing samples.

## References

- [1] Inoue A. Stabilization of metallic supercooled liquid and bulk amorphous alloys. *Acta Mater* 2000;48:279–306.
- [2] Wang WH, Dong C, Shek CH. Bulk metallic glasses. *Mater Sci Eng R* 2004;44: 45–89.
- [3] Schuh CA, Nieh TG. A nanoindentation study of serrated flow in bulk metallic glasses. *Acta Mater* 2003;51:87–99.
- [4] Inoue A, Zhang W, Zhang T, Kurodaka K. High-strength Cu-based bulk glassy alloys in Cu–Zr–Ti and Cu–Hf–Ti ternary systems. *Acta Mater* 2001;49:2645–52.
- [5] Pelletier JM. Influence of structural relaxation on atomic mobility in a  $Zr_{41.2}Ti_{13.8}Cu_{12.5}Ni_{10.0}Be_{22.5}$  (Vit1) bulk metallic glass. *J Non-Cryst Solids* 2008;354:3666–70.
- [6] Liu YT, Bhandari B, Zhou WB. Study of glass transition and enthalpy relaxation of mixtures of amorphous sucrose and amorphous tapioca starch syrup solid by differential scanning calorimetry (DSC). *J Food Eng* 2007;81:599–610.
- [7] Tombari E, Ferrari C, Johari GP, Shanker RM. Calorimetric relaxation in pharmaceutical molecular glasses and its utility in understanding their stability against crystallization. *J Phys Chem B* 2008;112:10806–14.
- [8] Aji DPB, Wen P, Johari GP. Memory effect in enthalpy relaxation of two metal–alloy glasses. *J Non-Cryst Solids* 2007;353:3796–811.
- [9] Badrinarayanan P, Simon SL, Lyng RJ, O'Reilly JM. Effect of structure on enthalpy relaxation of polycarbonate: experiments and modeling. *Polymer* 2008;49:3554–60.

- [10] Shin J, Nazarenko S, Phillips JP, Hoyle CE. Physical and chemical modifications of thiol-ene networks to control activation energy of enthalpy relaxation. *Polymer* 2009;50:6281–6.
- [11] Deubener J, Yue YZ, Bornhoft H, Ya M. Decoupling between birefringence decay, enthalpy relaxation and viscous flow in calcium borosilicate glasses. *Chem Geol* 2008;256:299–305.
- [12] Malek J, Svoboda R, Pustkova P, Cimanec P. Volume and enthalpy relaxation of a-Se in the glass transition region. *J Non-Cryst Solids* 2009;355:264–72.
- [13] Hodge IM, Berens AR. Effect of annealing and prior history on the enthalpy relaxation in glassy polymers. 5. Mathematical-Modeling of nonthermal preaging perturbations. *Macromolecules* 1985;18:1980–4.
- [14] Vigier G, Tatibouet J. Physical ageing of amorphous and semicrystalline poly (ethylene terephthalate). *Polymer* 1993;34:4257–66.
- [15] Perez J. Quasi-punctual defects in vitreous solids and liquid-glass transition. *Solid State Ionics* 1990;39:69–79.
- [16] Perez J. Defect diffusion model for volume and enthalpy recovery in amorphous polymers. *Polymer* 1988;29:483–9.
- [17] Gauthier C, Pelletier JM, David L, Vigier G, Perez J. Relaxation of non-crystalline solids under mechanical stress. *J Non-Cryst Solids* 2000;274:181–7.
- [18] Xu YL, Fang JX, Gleiter H, Hahn H, Li JG. Quantitative determination of free volume in Pd<sub>40</sub>Ni<sub>40</sub>P<sub>20</sub> bulk metallic glass. *Scripta Mater* 2010;62:674–7.
- [19] Haruyama O, Sakagami H, Nishiyama N, Inoue A. The free volume kinetics during structural relaxation in bulk Pd–P based metallic glasses. *Mater Sci Eng A* 2007;449–451:497–500.
- [20] Haruyama O, Inoue A. Free volume kinetics during sub-T<sub>g</sub> structural relaxation of a bulk Pd<sub>40</sub>Ni<sub>40</sub>P<sub>20</sub> metallic glass. *Appl Phys Lett* 2006;88:131906.
- [21] Haruyama O. Thermodynamic approach to free volume kinetics during isothermal relaxation in bulk Pd–Cu–Ni–P<sub>20</sub> glasses. *Intermetallics* 2007;15:659–62.
- [22] Haruyama O, Kohda M, Nishiyama N, Egami T. Volume relaxation in ternary bulk Pd– and Pt–P based metallic glasses. *J Phys Conf Ser* 2009;144:012050.
- [23] Haruyama O, Yamada S. Density and enthalpy relaxation behavior in a bulk Pd<sub>40</sub>Ni<sub>40</sub>P<sub>20</sub> metallic glass. *Mater Sci Forum* 2007;561–565:1283–6.
- [24] Haruyama O, Yokoyama Y, Kimura HM, Inoue A, Nishiyama N. Relaxation kinetics of bulk metallic glasses below glass transition temperature. *Mater Sci Forum* 2007;539–543:2059–64.
- [25] Yuan ZZ, Bao SL, Lu Y, Zhang DP, Yao L. A new criterion for evaluating the glass-forming ability of bulk glass forming alloys. *J Alloys Compd* 2008;459:251–60.
- [26] Chen QJ, Shen J, Zhang DL, Fan HB, Sun JF, McCartney DG. A new criterion for evaluating the glass-forming ability of bulk metallic glasses. *Mater Sci Eng A* 2006;433:155–60.
- [27] Lin LZ, Wei HQ, Ding YH, Zhang P, Xie GQ, Inoue A. A new criterion for predicting the glass-forming ability of bulk metallic glasses. *J Alloys Compd* 2009;475:207–19.
- [28] Liu L, Wu ZF, Zhang J. Crystallization kinetics of Zr<sub>55</sub>Cu<sub>30</sub>Al<sub>10</sub>Ni<sub>5</sub> bulk amorphous alloy. *J Alloys Compd* 2002;339:90–5.
- [29] Keryvin V, Vaillant ML, Rouxel T, Huger M, Gloriant T, Kawamura Y. Thermal stability and crystallisation of a Zr<sub>55</sub>Cu<sub>30</sub>Al<sub>10</sub>Ni<sub>5</sub> bulk metallic glass studied by in situ ultrasonic echography. *Intermetallics* 2002;10:1289–96.
- [30] Castellero A, Bossuyt S, Stoica M, Deledda S, Eckert J, Chen GZ, et al. Improvement of the glass-forming ability of Zr<sub>55</sub>Cu<sub>30</sub>Al<sub>10</sub>Ni<sub>5</sub> and Cu<sub>47</sub>Ti<sub>34</sub>Zr<sub>11</sub>Ni<sub>8</sub> alloys by electro-deoxidation of the melts. *Scripta Mater* 2006;55:87–90.
- [31] Haruyama O, Nakatama Y, Wada R, Tokunaga H, Okada J, Ishikawa T, et al. Volume and enthalpy relaxation in Zr<sub>55</sub>Cu<sub>30</sub>Ni<sub>5</sub>Al<sub>10</sub> bulk metallic glass. *Acta Mater* 2010;58:1829–36.
- [32] Slipenyuk A, Eckert J. Correlation between enthalpy change and free volume reduction during structural relaxation of Zr<sub>55</sub>Cu<sub>30</sub>Al<sub>10</sub>Ni<sub>5</sub> metallic glass. *Scripta Mater* 2004;50:39–44.
- [33] Pelletier JM, Van de Moortèle B. Phase separation and crystallization in the Zr<sub>41.2</sub>Ti<sub>13.8</sub>–Cu<sub>12.5</sub>–Ni<sub>10</sub>–Be<sub>22.5</sub> bulk metallic glass determined by physical measurements and electron microscopy. *J Non-Cryst Solids* 2003;325:133–41.
- [34] Zhang Y, Hann H. Study of the kinetics of free volume in Zr<sub>45.0</sub>Cu<sub>39.3</sub>Al<sub>7.0</sub>Ag<sub>8.7</sub> bulk metallic glasses during isothermal relaxation by enthalpy relaxation experiments. *J Non-Cryst Solids* 2009;355:2616–21.
- [35] Zhang T, Ye F, Wang YL, Lin JP. Structural relaxation of La<sub>55</sub>Al<sub>25</sub>Ni<sub>10</sub>Cu<sub>10</sub> bulk metallic glass. *Metall Mater Trans A* 2008;39A:1953–7.
- [36] Raghavan R, Murali P, Ramamurthy U. Influence of cooling rate on the enthalpy relaxation and fragility of a metallic glass. *Metall Mater Trans A* 2008;39A:1573–7.
- [37] Han TK, Zhang T, Inoue A, Yang YS, Kim IB, Kim YH. Thermal and mechanical properties of amorphous Zr<sub>65</sub>Al<sub>7.5</sub>Ni<sub>10</sub>Cu<sub>12.5</sub>Ag<sub>5</sub> alloy containing nanocrystalline compound particles. *Mater Sci Eng A* 2001;304–306:892–6.
- [38] Hodge IM. Effects of annealing and prior history on enthalpy relaxation in glassy polymers. 4. Comparison of five polymers. *Macromolecules* 1983;16:898–902.
- [39] Böhmer R, Ngai KL, Angell CA, Plazek DJ. Nonexponential relaxations in strong and fragile glass formers. *J Chem Phys* 1993;99:4201–9.
- [40] Gallino I, Shah MB, Busch R. Enthalpy relaxation and its relation to the thermodynamics and crystallization of the Zr<sub>58.5</sub>Cu<sub>15.6</sub>Ni<sub>12.8</sub>Al<sub>10.3</sub>Nb<sub>2.8</sub> bulk metallic glass-forming alloy. *Acta Mater* 2007;55:1367–76.
- [41] Zhang Y, Hann H. Quantification of the free volume in Zr<sub>45.0</sub>Cu<sub>39.3</sub>Al<sub>7.0</sub>Ag<sub>8.7</sub> bulk metallic glasses subjected to plastic deformation by calorimetric and dilatometric measurements. *J Alloys Compd* 2009;488:65–71.
- [42] Wen P, Zhao DQ, Pan MX, Wang WH, Shui JP, Sun YP. Relaxation behaviors of bulk metallic glass forming Zr<sub>46.75</sub>Ti<sub>8.25</sub>Cu<sub>7.5</sub>Ni<sub>10.0</sub>Be<sub>27.5</sub> alloy. *Intermetallics* 2004;12:1245–9.
- [43] Moynihan CT, Eastale AJ, Debolt MA, Tucker J. Dependence of the fictive temperature of glass on cooling rate. *J Am Ceram Soc* 1976;59:12–6.
- [44] Narayanaswamy OS. A model of structural relaxation in glass. *J Am Ceram Soc* 1971;54:491–7.
- [45] Wang XD, Jiang JZ, Yi S. Reversible structural relaxation and crystallization of Zr<sub>62</sub>Al<sub>8</sub>Ni<sub>13</sub>Cu<sub>17</sub> bulk metallic glass. *J Non-Cryst Solids* 2007;353:4157–61.
- [46] Martin SW, Walleiser J, Karthikeyan A, Sordelet D. Enthalpy relaxation studies of the glass transition in a metallic glass. *J Non-Cryst Solids* 2004;349:347–54.
- [47] Svoboda R, Pustkova P, Malek J. Relaxation behavior of glassy selenium. *J Phys Chem Sol* 2007;68:850–4.
- [48] Svoboda R, Honcova P, Malek J. Apparent activation energy of structural relaxation for Se<sub>70</sub>Te<sub>30</sub> glass. *J Non-Cryst Solids* 2010;356:165–8.
- [49] Wang JF, Liu L, Xiao JZ, Zhang T, Wang BY, Zhou CL, et al. Ageing behaviour of Pd<sub>40</sub>Cu<sub>30</sub>Ni<sub>10</sub>P<sub>20</sub> bulk metallic glass during long-time isothermal annealing. *J Phys D Appl Phys* 2005;38:946–9.
- [50] Lopez-Alemay PL, Vazquez J, Villares P, Jimenez-Garay R. A kinetic study on non-isothermal crystallization of the glassy alloy Sb<sub>0.16</sub>As<sub>0.43</sub>Se<sub>0.41</sub>. *J Non-Cryst Solids* 2000;274:249–56.
- [51] Wang J, Kou HC, Li JS, Gu XF, Xing LQ, Zhou L. Determination of kinetic parameters during isochronal crystallization of Ti<sub>40</sub>Zr<sub>25</sub>Ni<sub>6</sub>Cu<sub>9</sub>Be<sub>18</sub> metallic glass. *J Alloys Compd* 2009;479:835–9.
- [52] Park ES, Lee JY, Kim DH, Gebert A, Schutlz L. Correlation between plasticity and fragility in Mg-based bulk metallic glasses with modulated heterogeneity. *J Appl Phys* 2008;104:023520.
- [53] Bayri N, Izgi T, Gencer H, Sovak P, Gunes M, Atalay S. Crystallization kinetics of Fe<sub>73.5-x</sub>Mn<sub>x</sub>Cu<sub>1</sub>Nb<sub>3</sub>Si<sub>13.5</sub>B<sub>9</sub> (x = 0, 1, 3, 5, 7) amorphous alloys. *J Non-Cryst Solids* 2009;355:12–6.
- [54] Fernández R, Carrasco W, Zúñiga A. Structure and crystallization of amorphous Cu–Zr–Al powders. *J Non-Cryst Solids* 2010;356:1665–9.
- [55] Zhao L, Jia HL, Xie SH, Zeng XR, Zhang T, Ma CL. A new method for evaluating structural stability of bulk metallic glasses. *J Alloys Compd* 2010;504: S219–21.
- [56] Angell CA. Formation of glasses from liquids and biopolymers. *Nature* 1995;267:1924–35.
- [57] Park ES, Na JH, Kim DH. Correlation between fragility and glass-forming ability/plasticity in metallic glass-forming alloys. *Appl Phys Lett* 2007;91: 031907.
- [58] Cernoskova E, Cernosek Z, Holubova J, Frumar M. Structural relaxation near the glass transition temperature. *J Non-Cryst Solids* 2001;284:73–8.
- [59] Jeong HT, Fleury E, Kim WT, Kim DH, Hono K. Study on the mechanical relaxations of a Zr<sub>36</sub>Ti<sub>24</sub>Be<sub>40</sub> amorphous alloy by time-temperature superposition principle. *J Phys Soc Jpn* 2004;73:3192–7.
- [60] Fan GF, Löffler JF, Wunderlich RK, Fecht HJ. Thermodynamics, enthalpy relaxation and fragility of the bulk metallic glass-forming liquid Pd<sub>43</sub>Ni<sub>10</sub>Cu<sub>27</sub>P<sub>20</sub>. *Acta Mater* 2004;52:667–74.
- [61] Pauly S, Lee MH, Kim DH, Kim KB, Sordelet DJ, Eckert J. Crack evolution in bulk metallic glasses. *J Appl Phys* 2009;106:103518.
- [62] Takeuchi A, Kato H, Inoue A. Vogel–Fulcher–Tammann plot for viscosity scaled with temperature interval between actual and ideal glass transitions for metallic glasses in liquid and supercooled liquid states. *Intermetallics* 2010;18:406–11.
- [63] Kato H, Wada T, Hasegawa M, Saida J, Inoue A, Chen HS. Fragility and thermal stability of Pt- and Pd-based bulk glass forming liquids and their correlation with deformability. *Scripta Mater* 2006;54:2023–7.
- [64] Qin Q, Mckenna GB. Correlation between dynamic fragility and glass transition temperature for different classes of glass forming liquids. *J Non-Cryst Solids* 2006;352:2977–85.
- [65] Aken B, van de Hey P, Sietsma J. Structural relaxation and plastic flow in amorphous La<sub>50</sub>Al<sub>25</sub>Ni<sub>25</sub>. *Mater Sci Eng A* 2000;278:247–54.